Nondispersive-to-dispersive charge-transport transition in disordered molecular solids

P. M. Borsenberger*
Office Imaging Division, Eastman Kodak Company, Rochester, New York 14650-1714

L. T. Pautmeier and H. Bässler
Fachbereich Physikalische Chemie und Zentrum fur Materialwissenschaften der Philipps-Universitat, D-3550 Marburg, Germany

(Received 25 March 1992; revised manuscript received 2 July 1992)

The transition from nondispersive to dispersive charge transport at low temperatures is studied on *p*-diethylaminobenzaldehyde diphenyl hydrazone and by computer simulation. It is shown that the concept of hopping in a Gaussian density-of-states distribution provides a consistent framework for data analysis. Variation of time-of-flight current transients with sample thickness and temperature can quantitatively be accounted for in terms of the energetic disorder parameters inferred from nondispersive transport data. It is shown that deviations from scaling behavior is a signature of dispersive hopping in a Gaussian density-of-states distribution.

I. INTRODUCTION

In crystalline semiconductors or insulators, the field-driven motion of an initially δ-shaped packet of excess charge carriers gives rise to a constant displacement current. The current remains constant until the carriers have reached the electrode. Diffusive spreading of the carrier packet causes some broadening of the leading edge of the time-of-flight current transient. With disordered media, transients often do not exhibit plateaus. Inflection points, indicative of the arrival of carriers at an electrode, can only be distinguished by plotting the time dependence of the current on a double logarithmic scale.[1,2] The explanation of this behavior, originally proposed by Scher and Lax[3] and Scher and Montroll,[4] is that the mean velocity of the carriers decreases continuously and the packet spreads anomalously with time, if the time required to establish dynamic equilibrium exceeds the average transit time.

The Scher-Montroll concept[5,6] rests on the idea that the effect of disorder, considered to be the origin of the anomalies, can be modeled in terms of the continuous-time–random-walk formalism in which all of the disorder is cast into a waiting time distribution of the form $\Psi(t) \propto t^{-(1+\alpha)}$. Here, α is the dispersion parameter $0<\alpha<1$. The tacit assumption in the original work was that $\Psi(t)$ originates from the positional disorder of the hopping sites. In that case, however, the dispersion in transients should be temperature independent, contrary to experimental results in most disordered molecular solids. Moreover, both analytic[7,8] as well as simulation[9,10] studies indicated that dispersive transients in samples of macroscopic dimensions required a degree of positional disorder difficult to reconcile with the moderate variation of intersite distances in disordered molecular solids.

An alternative explanation is that dispersion derives from energy disorder that translates into a distribution of thermally activated transition rates. In fact, the assumption that an ensemble of carriers temporarily localized in an exponential distribution of trapping sites (realized, e.g., in amorphous chalcogenides) communicates with delocalized states above a mobility edge was shown to provide a consistent framework for explaining a diversity of experimental observations.[11–17] The multiple trapping concept has also been applied to poly(*N*-vinylcarbazole). On this basis, Müller-Horsche, Haarer, and Scher[18] inferred a distribution of detrapping rates from a Laplace transform of the temporal features of the current transients. However, such an analysis is meaningful only if (1) trap-to-trap migration can be neglected, and (2) transport occurs in an energetically well-defined transport level such as a valence or conduction band or an isoenergetic array of hopping sites. The latter assumption is all but straightforward. The inhomogeneous broadening of optical-absorption spectra of organic glasses and polymers is an unambiguous signature of the splitting of the exciton band into a manifold of localized states.[19] By analogy, the same should hold for charge-transport states. In that case, the above determination of trap release rates would be correct only if the width of the manifold of transport states was much narrower than that of the trap distribution. Previous optical studies argue against this notion.[20]

On the other hand, analytic[21] and simulation[22] studies provide evidence that hopping within an intrinsic distribution of hopping states (DOS) gives rise to dispersive transport even in the absence of traps. For these conditions, the degree of dispersion as well as the onset time relative to the transit time depend on $\hat{\sigma}$, the width of the DOS relative to kT. In previous simulation studies,[23] a simple criterion was developed for the occurrence of a transition form nondispersive to dispersive transport. Although qualitatively confirmed by numerous studies on allegedly trap-free materials, these experiments typically yield lower transition temperatures, equivalent to a lower

degree of energetic disorder, than predicted on the basis of the temperature dependence of the mobility. This could indicate that part of the measured thermal activation is due to a process other than disorder-controlled hopping. A possibility is polaron formation.[24–26] Alternatively, the discrepancy between experiment and theory could be related to the somewhat arbitrary definition of the establishment of dynamic equilibrium and/or the limited sample size in previous simulations.

In order to clarify this question and delineate the key features of dispersive transport in a material with a Gaussian DOS, a study of the transition from nondispersive to dispersive transport, henceforth $ND \rightarrow D$, has been conducted combining both Monte Carlo simulations and experiment. The material selected for this study was *p*-diethylaminobenzaldehyde diphenylhydrazone (DEH). This compound was chosen for two reasons: (1) amorphous films can be readily prepared by vapor deposition techniques, thus eliminating the very considerable effects of a polymer host; and (2) previous studies have shown that the effect of positional disorder can be neglected.[27] Apart from demonstrating that intrinsic energetic disorder is indeed sufficient to account for the observed effects, criteria will be presented for the analysis of dispersive transients in molecularly doped polymers.

II. MONTE CARLO SIMULATIONS

A. Procedures

The Monte Carlo simulations were based on a well-tested algorithm described previously.[22] A cubic sample with lattice constant $a = 6$ Å was used for the computations. The sample consisted of 70×70 sites in the x and y direction with periodic boundary conditions and up to 8000 sites in the z direction, which is the direction of the applied field. This is equivalent to a maximum sample length of 4.8 μm. Disorder was simulated by assigning site energies taken from a Gaussian distribution of standard deviation σ, yielding an energetic (diagonal) disorder parameter $\hat{\sigma} = \sigma / kT$. Positional disorder of the hopping sites has been ignored in order to keep the computation times at large $\hat{\sigma}$ within tolerable limits. We consider this neglect unimportant because with materials of practical interest, time-of-flight broadening of the current transient is dominated by energetic disorder and will be more so the larger $\hat{\sigma}$ becomes.[28] The carriers were started randomly in energy and their random walk followed under the influence of a constant field of 6×10^5 V/cm. Hopping was assumed to be controlled by jump rates of the Miller-Abrahams type,

$$\nu_{ij} = \nu_0 \exp - \left[2\gamma a \frac{\Delta R_{ij}}{a} \right] \begin{cases} \exp - \dfrac{(\varepsilon_j - \varepsilon_i)}{kT}, & \varepsilon_j > \varepsilon_i \\ 1, & \varepsilon_j < \varepsilon_i \end{cases} \quad (1)$$

ignoring polaronic effects. Typically 100–150 carriers per parameter set were started independently and a new sample configuration was set up after every 20 carriers. The computations yielded transients as well as the mean carrier arrival times, parametric in $\hat{\sigma}$ and the number of lattice planes, n_z, in the field direction.

B. Results

A family of current transients, parametric in $\hat{\sigma}$, is shown in Fig. 1 for a sample with $n_z = 4000$, equivalent to a thickness of 2.4 μm. The occurrence of a $ND \rightarrow D$ transition with increasing $\hat{\sigma}$ is obvious. While the transients reveal a plateau of variable temporal length for $\hat{\sigma} < 4$, this is no longer the case for $\hat{\sigma} > 4.4$. To delineate the general phenomenological pattern, a series of double logarithmic plots, parametric in $\hat{\sigma}$, covering up to 20 decades in time and up to 10 decades in amplitude are presented in Fig. 2. The curves for $\hat{\sigma} = 3$, 6, and 8 represent the results of an analytic effective-medium (EMA) calculation of the zero-field diffusivity of a packet of carriers in an infinite sample.[21] Apart from demonstrating the mutual consistency of EMA and simulation results, these plots indicate that in no case a simple power law of the type $i(t) \propto t^{-(1-\alpha)}$ is obeyed for times less than the mean arrival time $\langle t_T \rangle$. At short times, the time dependence of the current is virtually independent of $\hat{\sigma}$ and tends to saturate earlier with decreasing $\hat{\sigma}$.

Reducing the sample length at fixed $\hat{\sigma}$ causes the initial portion of the transients to appear more dispersive. This is shown in Fig. 3. The $ND \rightarrow D$ transition is more clearly delineated by plotting the reciprocal mean carrier arrival time as a function of $\hat{\sigma}^2$, parametric in sample

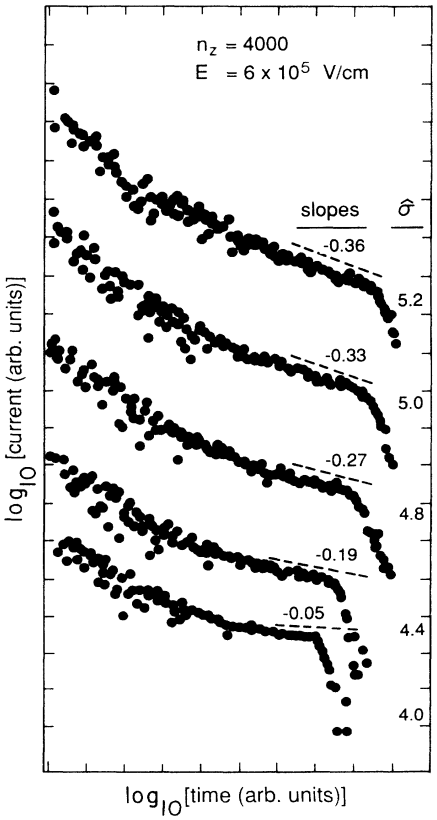

FIG. 1. Simulated transients, parametric in $\hat{\sigma}$.

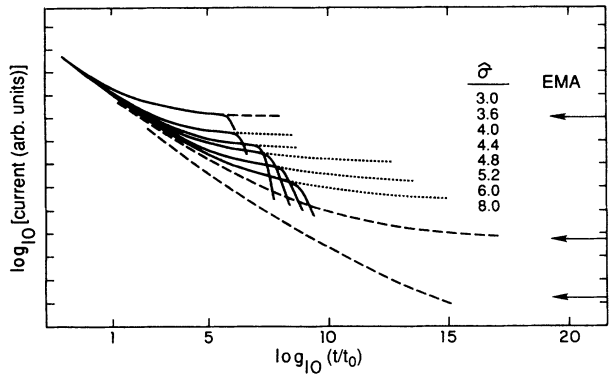

FIG. 2. Double logarithmic current vs time plots. The full and dotted curves are simulation results. Their extrapolation toward the equilibrium dashed curves are the results of the effective-medium approximation for an infinite sample.

length and the arrival time as a function of n_z, at variable $\hat{\sigma}$, as shown in Figs. 4 and 5, respectively. Within the dispersive regime, $t_T(n_z)$ deviates from linearity, $\langle t_T \rangle \propto n_z^m$, where $1.25 < m < 1.40$ for $4.0 < \hat{\sigma} < 5.2$. At the same time, $d/E\langle t_T \rangle$ exceeds the value predicted by the dependence of the mobility on the disorder parameter at moderate fields,[29]

$$\mu(\hat{\sigma}) = \mu_0 \exp - \left[\frac{2\hat{\sigma}}{3} \right]^2 . \quad (2)$$

Instead, $\langle t_T \rangle^{-1}$ approximately varies as $\exp -(\hat{\sigma}/2)^2$. In

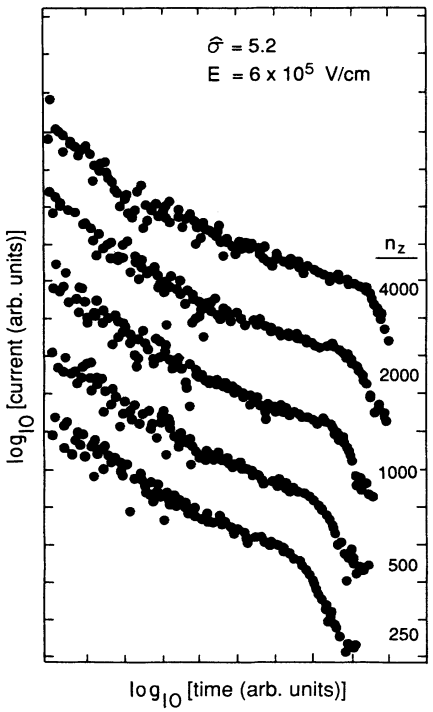

FIG. 3. Simulated transients, parametric in sample length, expressed by the number of lattice planes in the field direction.

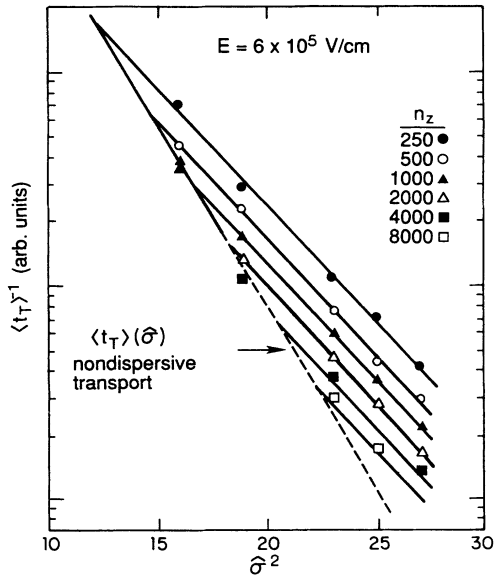

FIG. 4. Simulated reciprocal mean arrival times vs $\hat{\sigma}^2$, parametric in the number of lattice planes. The asymptote describing nondispersive transport was taken from Ref. 29.

previous studies, the onset of dispersion has been defined by the condition that the current no longer decays to a true plateau value for $t < \langle t_T \rangle$. Operationally, the time at which the current becomes time dependent turned to be about one tenth of the time a packet of carriers needs to equilibrate energetically within a Gaussian DOS.[23] Figure 4 offers a criterion for the occurrence of the $ND \rightarrow D$ transition that alleviates the problem of having to define the time at which the current becomes constant. It indicates that below a critical value of the disorder pa-

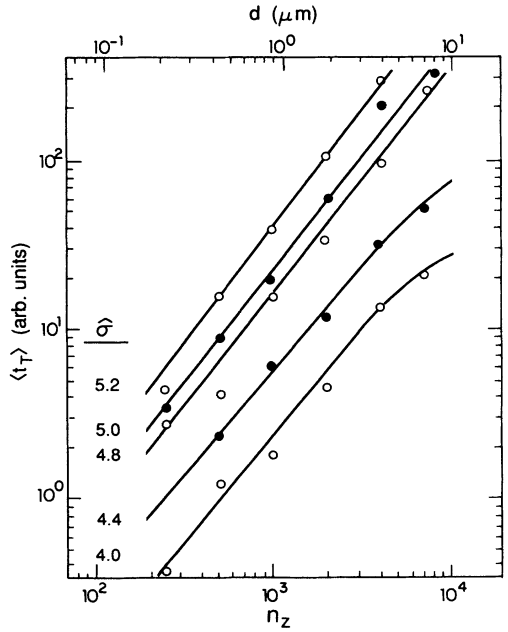

FIG. 5. Mean arrival times vs n_z, parametric in $\hat{\sigma}$.

rameter, $\hat{\sigma}_c$, the mobility derived from the mean carrier arrival time is independent of thickness, thus reflecting a genuine material property. In this sense, the $ND \rightarrow D$ transition is a transition between a transport regime in which the mean carrier arrival time yields a transport coefficient, i.e., mobility, that is independent of thickness and a regime in which this is no longer the case. Operationally, the $ND \rightarrow D$ transition can be defined via the intersection of the log $\langle t_T \rangle$ versus $\hat{\sigma}^2$ lines representing the average reciprocal carrier arrival times in the nondispersive and dispersive regimes, respectively. This yields a correlation between the critical disorder parameter $\hat{\sigma}_c$ and the sample length. Principally, the same information can be extracted from a plot of $\langle t_T \rangle$ versus the sample length. Hence $\hat{\sigma}_c(d)$ is inferred from the sample length at which the extrapolated $\langle t_T \rangle$ versus d line intersects the $\langle t_T \rangle = \mu E/d$ line, characterizing ND behavior. Figure 6 indicates that the critical disorder parameter at which the $ND \rightarrow D$ transition occurs increases with the number of lattice planes as

$$\hat{\sigma}_c^2 = A + B \log_{10} n_z \ , \tag{3}$$

where $A = -3.6$ and $B = 6.7$ are empirical constants, equivalent to $\hat{\sigma}_c^2 = A' + B \log_{10} L$, where $A' = 44.8$ and L is the sample thickness in cm. With a thickness of 20 μm and a DOS 0.1 eV, transients are then predicted to be dispersive at 232 K. According to the criterion used earlier, a temperature of 286 K would have been estimated.

A transient at $\hat{\sigma} = \hat{\sigma}_c$ does reveal an inflection if plotted on a double linear scale, yet not a well-developed plateau. This is illustrated in Fig. 7, showing a transient for $n_z = 8000$ at $\hat{\sigma} = 4.8$ which is very close to $\hat{\sigma}_c$, as shown in Fig. 6. Obviously, transients that appear moderately dispersive on double linear scales featuring a slope $-(1-\alpha_1) \simeq 0.27$ in double logarithmic representation are still satisfactory for determining mobilities that represent bulk properties. The reason is that the inflection monitors the arrival of the fastest carriers equilibrating earlier, while residual current relaxation is controlled by slower carriers hopping within the bottom part of the occupational DOS. Figure 7(a) also illustrates that the absolute magnitude of the mobility may differ up to a factor of 2, depending on how the arrival time is defined. Inferring $\langle t_T \rangle$ from the intersection of asymptotes in double linear plots, which is the common experimental technique, yields values that are approximately a factor of 2 larger than values derived from $\langle t_T \rangle$ which, unfortunately, are not directly accessible in experiment. Another reason why σ_c is larger than previously assumed is related to the effect an electric field has on the relaxation behavior of carriers within a Gaussian DOS. A field raises the equilibrium energy of carriers within the DOS and, concomitantly, shortens the equilibrium time.

III. EXPERIMENT

The molecular structure of DEH is shown in Fig. 8. A slurry of sodium acetate (13.5 mmol) and 1,1-

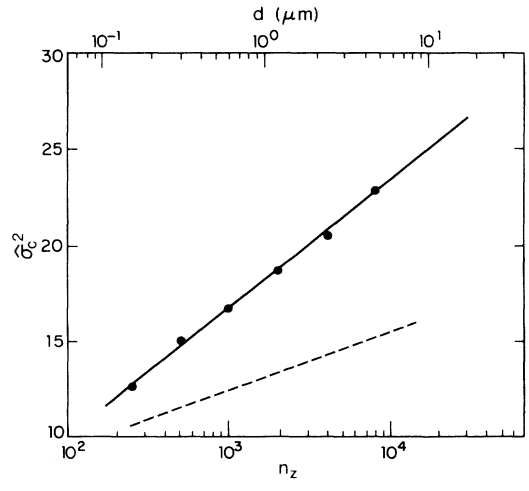

FIG. 6. The disorder parameter $\hat{\sigma}_c^2$ at which the $ND \rightarrow D$ transition occurs vs sample length. The dashed line was obtained from Ref. 22.

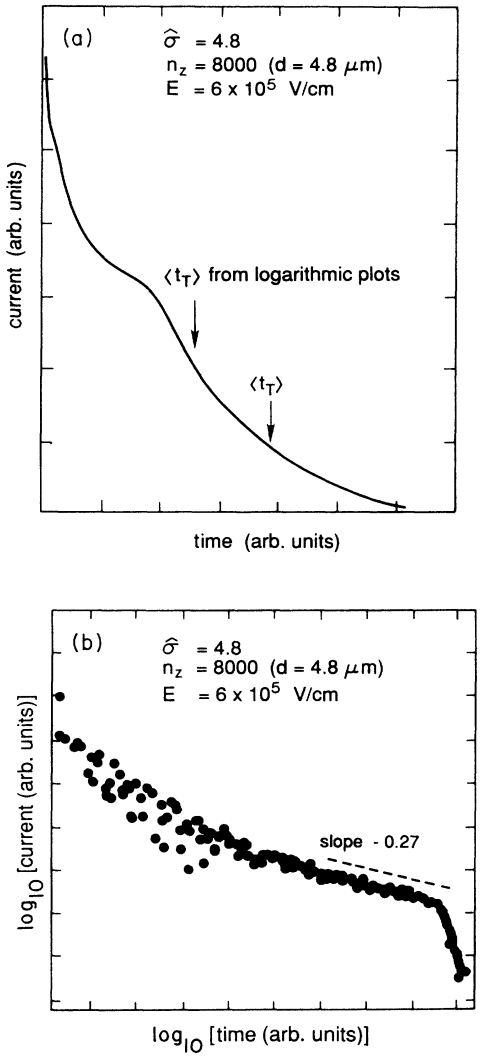

FIG. 7. Simulated transients at the $ND \rightarrow D$ transition in (a) double linear and (b) double logarithmic representation.

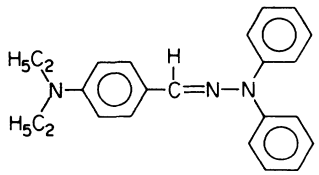

FIG. 8. The molecular structure of *p*-diethylaminobenzaldehyde-diphenyl hydrazone (DEH).

diphenylhydrazine hydrochloride (13.5 mmol) in water (50 mL) was added to a refluxing mixture of ethanol (100 mL) and *p*-diethylaminobenzaldehyde (10 mmol). After 2.5-h reflux, the reaction was cooled in ice, filtered with aqueous ethanol and water, then dried under vacuo to a 61% yield of DEH. The molecular weight and density of DEH are 343 g/mol and 1.17 g/cm^3. The glass transition and melting temperatures are 280 and 360 K, respectively. The relative dielectric constant is 3.06. Films of this compound were prepared by thermal sublimation onto a NESA (SnO) coated quartz substrate previously coated with a 0.10-μm layer of α-Se. Sublimation was from a Ta crucible at 340 K. For a crucible-to-substrate distance of 30 cm, this gave a deposition rate of approximately 200 Å/s. The background pressure was less than 10^{-7} Torr. From cross-section photomicrographs and capacitance measurements, the thickness was 5.6 μm. Finally, a 0.05-μm Au electrode was deposited on the surface of the DEH layer. During the deposition processes, the substrate was attached to a liquid N_2 cooled stage. Samples deposited on room-temperature substrates were invariably polycrystalline. Films prepared in the above manner were amorphous with no indications of crystallization over a period of several weeks.

The mobility measurements were by conventional time-of-flight (TOF) techniques. By this method, the displacement of a sheet of holes injected into the DEH layer from a photoemitting α-Se layer is time resolved. Photoexcitation was by 3-ns exposure of 440 nm radiation derived from a dye laser. The exposures were filtered such that the charge injected into the DEH layer was less than 0.05 CV_0. The photocurrent transients were measured with a Tektronix model 2301 transient digitizer system. All measurements were made in air. Figure 9 shows a

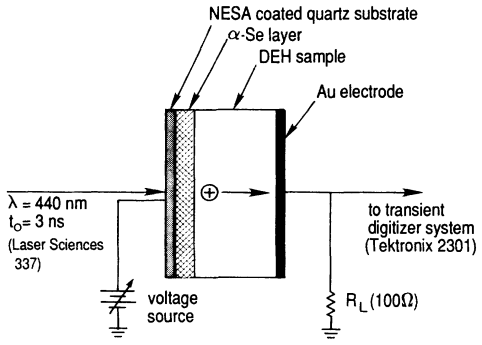

FIG. 9. A schematic of the experimental apparatus.

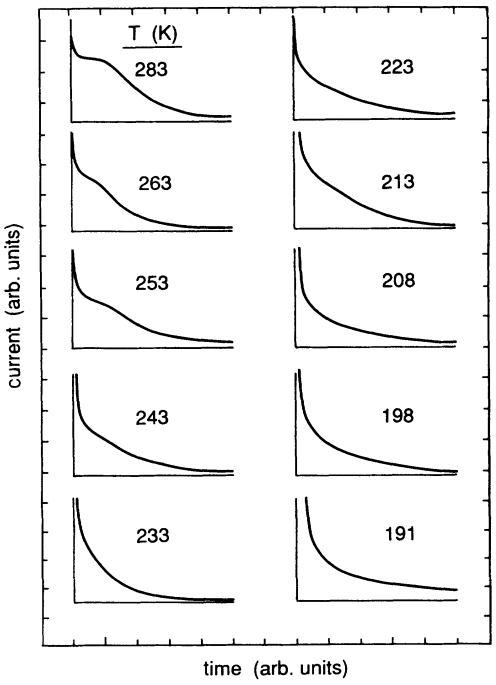

FIG. 10. Experimental transients, parametric in temperature, measured at 6×10^5 V/cm.

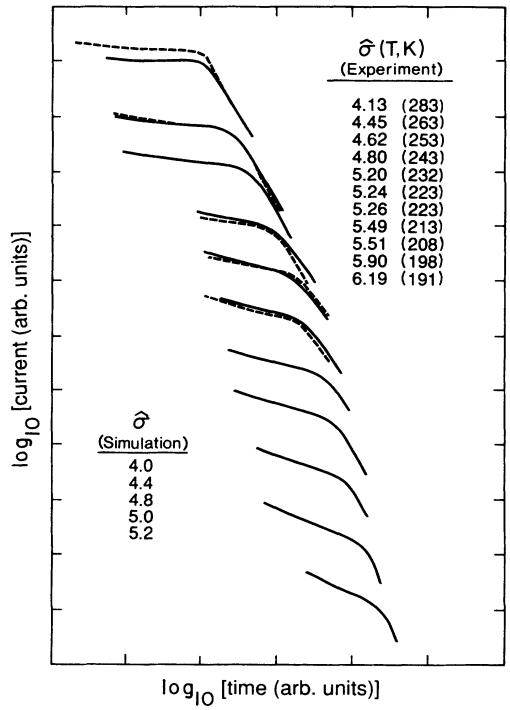

FIG. 11. Comparison between experimental (full curves) and simulated (dashed) transients. The field was 6×10^5 V/cm. The simulations are for $n_z=8000$, except for $\hat{\sigma}=5.2$ which has been extrapolated from the data for $n_z\leq4000$. The experimental transient for $\hat{\sigma}=4.45$ is coincident with the simulation for $\hat{\sigma}=4.4$.

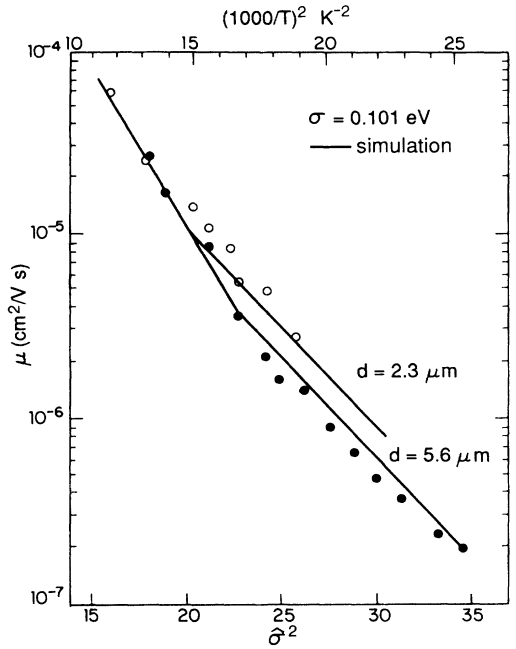

FIG. 12. Hole mobilities in DEH evaluated from the relationship $\mu=d/E\langle t_T\rangle$. Here $\langle t_T\rangle$ has been determined from the intersection of the asymptotes in either the double linear or the double logarithmic representation.

schematic of the experimental apparatus. A more detailed description of the experimental techniques has been given elsewhere.[29,30]

IV. RESULTS

A series of transients measured with a 5.6-μm sample at various temperatures is shown in Fig. 10 in double linear and in Fig. 11 in double logarithmic representation. The transition from what is conventionally termed nondispersive to strongly dispersive behavior is obvious.

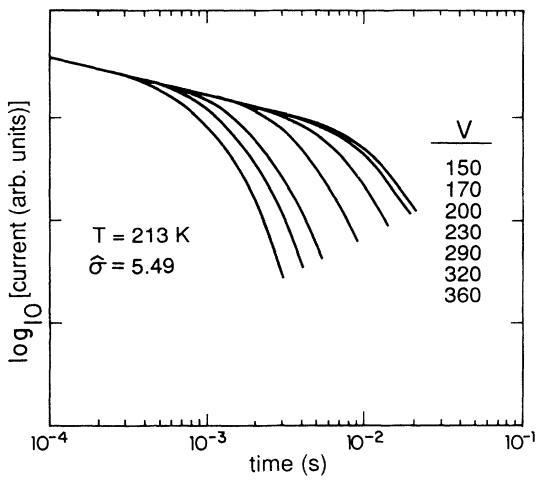

FIG. 13. Experimental transients, parametric in voltage. The plots are normalized to the arrival time at short times.

In Fig. 12, the mobility determined from the intersection of asymptotes in either double linear or double logarithmic representation is shown as a function of temperature. Earlier data[27] obtained with a 2.3-μm sample are included for comparison. The consistency with the present data in the nondispersive regime is an illustration of the reproducibility of both sample preparation and experiment. A family of transients, parametric in voltage at 213 K, is shown in Fig. 13.

V. DISCUSSION

The main purpose of this study is to clarify whether the occurrence of the $ND\rightarrow D$ transition, as revealed by time-of-flight transients that become featureless in double linear representation, can be rationalized by the concept of intrinsic disorder. The key parameters required for comparing experimental and computed transients are σ and Σ, characterizing diagonal and off-diagonal disorder, respectively.[29] In the case of DEH, the problem is simplified because the latter is negligibly small, as previous work has indicated.[27] The width of the DOS can be extracted from the temperature dependence of the mobility determined from nondispersive transients via Eq. (2). By comparing experimental and simulation data, $\sigma=0.101$ eV is determined. In Ref. 27, $\sigma=0.104$ was reported. This value, however, was extracted from the temperature dependence of the extrapolated zero-field mobility. This procedure slightly overestimates σ because it ignores the deviation of the mobility from an $\exp(\beta E^{1/2})$ law at low fields.[29] The difference, however, is on a percent level only. Having determined σ allows translating the temperature scale into a $\hat{\sigma}$ scale needed for comparing experiment and simulation. Figure 11 shows that within the limit of experimental resolution and, notably, accuracy of simulation data, the agreement is good. It is worth noting that the only adjustable parameter is the time scale of the simulation. A complementary consistency check is provided by a plot of the mobility versus $\hat{\sigma}^2$ for the sample thicknesses of 5.6 (present data) and 2.3 μm.[27] The results are shown in Fig. 12. The solid lines represent the simulation results for $E=6\times10^5$ V/cm and $L=2.3$ and 5.6 μm, respectively. Again, the only adjustable parameter is the absolute time scale of the simulations, chosen in such a way to ensure matching of the high-temperature data. Again, the agreement is good. It is particularly noteworthy that the predicted variation of $\hat{\sigma}_c$ with the sample length is verified. This is an unambiguous manifestation of the success of the disorder model to quantitatively account for TOF transients within a broad temperature range encompassing the $ND\rightarrow D$ transition temperature.

The implication of the above results concerning the role of polaronic effects in charge transport will be illustrated by a simple estimate. If one would plot the mobility data obeying Eq. (2) in an Arrhenius relationship, one would obtain an apparent temperature-dependent activation energy

$$\Delta_0=-k\frac{\partial\ln(\mu/\mu_0)}{\partial(1/T)}=\frac{8\sigma^2}{9kT}\ . \tag{4}$$

At $T=263$, $\sigma=0.101$ eV gives $\Delta_0=0.40$ eV. Assume that only one-half of the measured activation energy was due to disorder, the remaining being due to polaronic effects. Then the width of the DOS would be 0.071 eV. One would then expect the $ND \rightarrow D$ transition from thickness-independent to thickness-dependent transport to occur at 172 K, instead of 244 K as observed. Even a 10% polaronic contribution would depress the transition temperature by 14 K. We therefore reinforce the implication of previous work[27] that the polaronic contribution to the temperature dependence of the mobility in DEH cannot be much in excess of the uncertainty involved in determining σ, which is of order 3 meV. This is in accord with results for other materials.[30,31]

We now address the implication of the present results for the interpretation of dispersive transport in random organic media in more general terms. Dispersive transients are often analyzed in terms of the algebraic decay functions[4]

$$i(t) \propto \begin{cases} t^{-(1-\alpha)}, & t < t_T \\ t^{-(1+\alpha)}, & t > t_T \end{cases} . \tag{5}$$

This procedure has been shown to be appropriate when transport occurs by multiple trapping[12-17] or hopping[32] within an exponential distribution of trapping or hopping states provided that $T_0/T > 1$, T_0 being the slope parameter of the distribution.[33] Equation (5) is a consequence of the temporal course of energetic relaxation of carriers within the DOS. Because of the faster tailing of a Gaussian DOS, energetic relaxation is slower than an exponential DOS and dynamic equilibrium can finally be established. Unfortunately, replacement of an exponential by a Gaussian DOS renders the mathematical treatment intractable in analytical terms. Instead, one has to rely on approximate method such as the effective-medium treatment of Movaghar and co-workers,[21] or simulation. Their mutual consistency has meanwhile been demonstrated. As a consequence, the time dependencies of the mean energy of a packet of carriers and their diffusivity no longer can be cast into simple analytical expressions. The recognition that the excess diffusivity of carriers in the dispersive transport regime is to first order proportional to their rate of energetic relaxation does not provide a basis for data analysis either, since the latter quantity is not experimentally accessible.[34] The unfortunate consequence is that upon analyzing dispersive transients for disordered molecular solids known to feature a Gaussian-shaped DOS, one has to rely on numerical methods although the underlying stochastic processes are well understood.

From Fig. 2, the failure of Eq. (5) for rationalizing dispersive transients in a material with a Gaussian DOS is obvious. Operationally one can, nevertheless, determine a dispersion parameter from the current transient in double logarithmic representation within, say, the last one and a half decades in time prior to the inflection because the curvature is small on this time scale. Figure 14 presents experimental as well as simulation data for the related slope $-(1-\alpha_1)$ of the double logarithmic curves for $t < \langle t_T \rangle$. Empirically, $-(1-\alpha_1) \propto (\hat{\sigma}-3.9)^{3/4}$. This

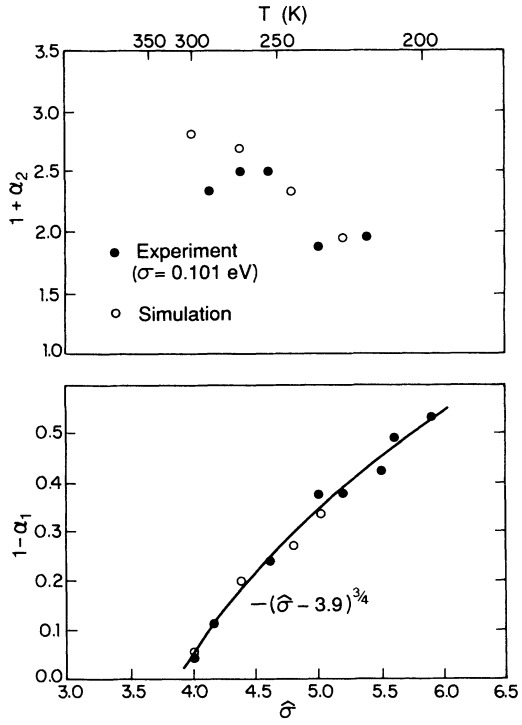

FIG. 14. Experimental (open circles) and simulated (solid circles) values for the slope parameters of Scher-Montroll plots.

relationship differs from that in earlier simulation work on samples consisting of 40 lattice planes only. In view of the limited sample size, only the initial portion of the relaxation processes could then be followed.[22]

The parameter α_1 may be used to characterize a dispersive transient, although it must not be considered as the dispersion parameter in the sense of Scher-Montroll (SM) theory, implying that it can be recovered from different functional dependencies. The failure of this procedure can be illustrated by the following argument.

(a) SM theory predicts[4] $\langle t_T \rangle \propto (d/E)^{1/\alpha}$. Simulated transients do, in fact, bear out a superlinear dependence of $\langle t_T \rangle$ on the sample length, as shown in Fig. 5. However, α values determined via Eq. (5) are larger than α_1.

(b) According to SM theory, slopes of double logarithmic plots should add to 2, implying that in the time domains $t \gtrsim \langle t_T \rangle$ the decay of the current is controlled by the same α. Figure 14 contradicts this prediction. Despite considerable data scatter, it is obvious that α_2, inferred from the tail of the double logarithmic plots, always exceeds α_1. This is a common observation, frequently encountered in analyzing dispersive transients in disordered molecular solids, and no general solution to the problem has been offered thus far. The present work demonstrates that is an inherent feature of dispersive transport in a Gaussian DOS. It is a signature of the failure of Eq. (5), in particular of the fact that the dispersion parameter is not a good statistical quantity for describing dispersive transport processes.

(c) The relationship $\langle t_T \rangle \propto (d/E)^{1/\alpha}$ implies that

within the dispersive regime the dependence of $\langle t_T \rangle$ on d and E should have the same exponent. In view of the very considerable increase in computational time with decreasing field at large $\hat{\sigma}$, we did not attempt to simulate the field dependence of $\langle t_T \rangle$. However, experiments on DEH at 213 K, i.e., $\hat{\sigma}=5.5$, show a $\langle t_T \rangle \propto E^m$ relationship with $m \simeq 2.5$. These results yield $\alpha=0.4$, as compared with $\alpha_1=0.55$ derived from the slope of the double logarithmic plots. The results are shown in Fig. 15.

These results demonstrate that the scaling behavior considered to be a hallmark of dispersive transport is not, except at best in zero-order approximation, fulfilled in the case of hopping within a Gaussian DOS. Scaling is the consequence of an algebraic waiting time distribution $\Psi(t) \propto t^{-(1+\alpha)}$, with α being independent of time. This is realized in materials in which multiple trapping within an exponential trap distribution prevails. Hopping within a Gaussian DOS, which is the signature of organic glasses and molecularly doped polymers, does not fall into this category. One can rationalize the violation of scaling in terms of the energy relaxation function. In the case of multiple trapping or, equivalently, hopping in an exponential DOS, energetic relaxation of an ensemble of excitation strictly follows a logarithmic time dependence, independent of the absolute time scale. Changing the experimental time scale by varying the sample thickness or the field will not, therefore, change the relaxation pattern. Concomitantly, current transients are universal on a double logarithmic scale. For a Gaussian DOS, the energy relaxation function is no longer linear on a logarithmic scale but tends to settle at a mean energy $-\sigma^2/kT$ below the center of the DOS. Changing the time scale by varying either the sample length or the field will therefore alter the relaxation pattern. Reducing the length will shift the relaxation pattern into a time domain in which $\partial \Delta E / \partial \ln t$ is larger, i.e., render the transients more dispersive. On the other hand, increasing the field will raise the mean equilibrium energy of carriers with the consequence that equilibrium is attained earlier.

The similarity between the transients presented herein and literature results of a wide range of molecularly doped polymers[7,35,36] suggests that the present explanation grasps the main elements of charge transport in the disordered molecular solid state. The ubiquitous strong temperature dependence of the transport parameters argues strongly in favor of the predominance of energetic disorder, as opposed to geometrical disorder involving tunneling among localized states or transport on fractal surfaces. On the other hand, the transients reported by Müller-Horsche, Haarer, and Scher[18] for poly(*N*-vinylcarbazole) exhibit a faster initial decay than predicted by the concept of solely intrinsic energetic disorder. The most likely reason for this discrepancy is the presence of structural traps, such as incipient dimers, providing another channel for carrier relaxation. In fact, previous[37] and more recent[38] simulations on large-size trap-containing samples indicated that the presence of traps does enhance the initial current decay. Since the concentrations of inadvertent physical and chemical traps depend on sample preparation, and in the case of poly(*N*-vinylcarbazole) on tacticity, it is all but surprising that transients measured in different laboratories on different samples differ in certain details while following the same general pattern. This pattern includes the occurrence of a transition from nondispersive to dispersive transport, the absence of rigorous universality, deviations from algebraic time dependencies, and the strong temperature dependence of the mean carrier arrival time.

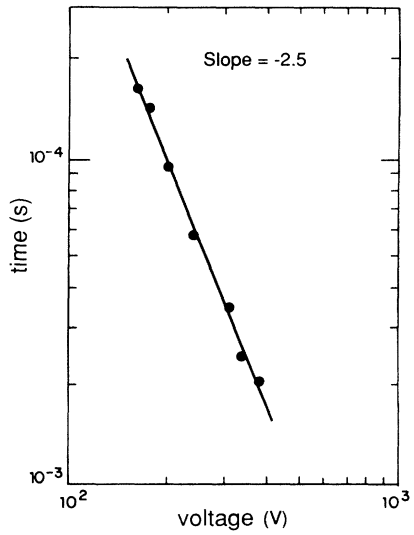

FIG. 15. The temporal shift of the transients of Fig. 13, parametric in the applied voltage.

VI. CONCLUSIONS

The present work substantiates the conclusion that the disorder parameter(s) of a material are of more fundamental importance than a heuristically defined dispersion parameter. Knowledge of the disorder parameters allows the establishment of a consistent microscopic interpretation for both dispersive and nondispersive transport. In this study, only energetic disorder has been considered. It has been shown that transients for a material with weak off-diagonal disorder can, in fact, be understood in quantitative albeit nonanalytic terms. Any effect of superimposed off-diagonal disorder needs to be delineated in future work.

ACKNOWLEDGMENTS

The authors would like to acknowledge the assistance of W. T. Gruenbaum for the preparation of the DEH and E. H. Magin for the mobility measurements. The financial support by the Deutsche Forschungsgemeinschaft and the Fond der Chemischen Industrie is also gratefully acknowledged.

*Author to whom correspondence should be addressed.

[1]J. Mort and G. Pfister, *Electronic Properties of Polymers,* edited by J. Mort and G. Pfister (Wiley, New York, 1982), p. 215.
[2]G. Pfister and H. Scher, Adv. Phys. **27**, 747 (1978).
[3]H. Scher and M. Lax, Phys. Rev. B **7**, 4491 (1973).
[4]H. Scher and E. W. Montroll, Phys. Rev. B **12**, 2455 (1975).
[5]M. F. Shlesinger, J. Stat. Phys. **10**, 421 (1974).
[6]J. Klafter and R. Silbey, Phys. Rev. Lett. **44**, 55 (1980).
[7]B. Movaghar and W. Schirmacher, J. Phys. C **14**, 589 (1981).
[8]B. Movaghar, B. Grünewald, B. Pohlmann, D. Würtz, and W. Schirmacher, J. Stat. Phys. **30**, 315 (1983).
[9]J. M. Marshall, Philos. Mag. B **47**, 323 (1983).
[10]B. Ries and H. Bässler, Phys. Rev. B **35**, 2295 (1987).
[11]M. E. Scharfe, Phys. Rev. B **2**, 5025 (1970).
[12]M. Silver and L. H. Cohen, Phys. Rev. B **15**, 3276 (1977).
[13]J. Noolandi, Phys. Rev. B **16**, 4466 (1977).
[14]F. Schmidlin, Phys. Rev. B **16**, 2362 (1977).
[15]T. Tiedje and A. Rose, Solid State Commun. **37**, 49 (1981).
[16]J. Orenstein and M. Kastner, Phys. Rev. Lett. **46**, 1421 (1981).
[17]V. Arkhipov and A. I. Rudenko, Philos. Mag. B **45**, 189 (1982).
[18]E. Müller-Horsche, D. Haarer, and H. Scher, Phys. Rev. B **35**, 1273 (1987).
[19]R. Jankowiak, K. D. Rockwitz, and H. Bässler, J. Phys. Chem. **87**, 552 (1983).
[20]U. Rauscher and H. Bässler, Macromolecules **23**, 398 (1990).
[21]B. Movaghar, M. Grünewald, B. Ries, H. Bässler, and D. Würtz, Phys. Rev. B **33**, 5545 (1986).
[22]G. Schönherr, H. Bässler, and M. Silver, Philos. Mag. B **44**, 47 (1981).
[23]L. Pautmeier, R. Richert, and H. Bässler, Philos. Mag. Lett. **59**, 325 (1989).
[24]L. B. Schein and J. X. Mack, Chem. Phys. Lett. **149**, 109 (1988).
[25]A. V. Vannikov, A. Yu Kryukov, A. G. Tyurin, and T. S. Zhuravleva, Phys. Status Solidi A **115**, K47 (1989).
[26]A. Peled, L. B. Schein, and D. Glatz, Phys. Rev. B **41**, 10 835 (1990).
[27]P. M. Borsenberger, Adv. Mater. Opt. Electron. **1**, 73 (1992).
[28]L. Pautmeier, R. Richert, and H. Bässler, Philos. Mag. B **63**, 587 (1991).
[29]P. M. Borsenberger, L. Pautmeier, and H. Bässler, J. Chem. Phys. **94**, 5447 (1991).
[30]P. M. Borsenberger, L. Pautmeier, R. Richert, and H. Bässler, J. Chem. Phys. **94**, 8276 (1991).
[31]P. M. Borsenberger, L. Pautmeier, and H. Bässler, J. Chem. Phys. **95**, 1258 (1991).
[32]M. Silver, G. Schönherr, and H. Bässler, Phys. Rev. Lett. **48**, 352 (1982).
[33]H. Schnörer, D. Haarer, and A. Blumen, Phys. Rev. B **38**, 8097 (1988).
[34]B. Ries, H. Bässler, M. Grünewald, and B. Movaghar, Phys. Rev. B **37**, 5508 (1988).
[35]G. Pfister and C. H. Griffith, Phys. Rev. Lett. **40**, 659 (1978).
[36]F. C. Bos and D. M. Burland, Phys. Rev. Lett. **58**, 152 (1987).
[37]M. Silver, G. Schönherr, and H. Bässler, Philos. Mag. B **43**, 943 (1981).
[38]A. Dieckmann (unpublished).

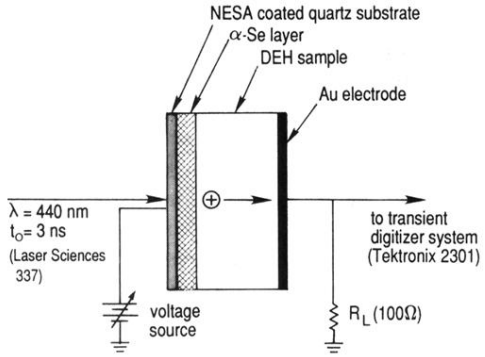

FIG. 9. A schematic of the experimental apparatus.